# Transport climatology of tropospheric ozone: Bermuda, 1988-1991

Jennie L. Moody,[1] Samuel J. Oltmans,[2] Hiram Levy II,[3] and John T. Merrill[4]

**Abstract.** We determined the major transport patterns for Bermuda and quantified the degree to which they influenced variability in ozone concentrations by applying cluster analysis to isentropic trajectories from September 1988, through September 1991. Concentration distributions of ozone associated with these transport patterns were significantly different. The highest concentrations of ozone in each season were associated with transport off the North American continent; the lowest concentrations were during low-level maritime transport around the Bermuda high. Using the vertical component of the isentropic trajectories, we also showed that the most extreme concentrations of ozone occurred with rapidly descending air from midtropospheric levels. This pattern was most pronounced in April and May when more than 50% of the $O_3$ variability was related to transport differences. We conclude that this relatively remote marine site, which normally experienced low maritime ozone levels ($\sim$30 parts per billion by volume (ppbv)), periodically entrained dry, ozone-rich ($\sim$55 ppbv) midtropospheric air in association with strong subsidence in high pressure behind spring low-pressure systems. Although the ultimate source of these midtroposphere, midlatitude, elevated-ozone concentrations is still being investigated, the synoptic meteorology associated with these transport patterns supports a significant contribution from the upper troposphere and lower stratosphere.

## Introduction

Tropospheric ozone is an important atmospheric oxidizing agent and plays a key role in the chemical transformations of many gases, aerosols, and hydrometeors [*Logan*, 1985; *Crutzen*, 1987]. A specific goal of the Atmosphere Ocean Chemistry Experiment (AEROCE) is to characterize the distribution of tropospheric ozone, to determine its role in photochemical processes over the North Atlantic, and to estimate the relative importance of continental and stratospheric sources and local production. In this paper we present a climatology of ozone measured on Bermuda between 1988 and 1991. We used trajectory model estimates of isentropic motion to quantify the impact of day-to-day variations in atmospheric transport on ozone variability.

From our experience in the AEROCE program and earlier research, it is clear that trajectories aid the interpretation of atmospheric chemical variability. An increasing number of references in the current literature couple trajectory calculations with chemical data. Trajectories are typically used as atmospheric tracers to determine potential source regions of sampled air. They may be taken individually to understand specific chemical signatures over short time periods [*Paluch et al.*, 1992; *Parrish et al.*, 1992] or they may be taken together (ensemble) to develop a climatology of large-scale atmospheric motion [*Miller et al.*, 1993].

*Oltmans and Levy* [1992], in their analysis of the AEROCE ozone data from Bermuda and Barbados, show that large variations in ozone concentration can be associated with abrupt changes in transport described by back trajectories. They subjectively define a relationship between the highest ozone values and transport from the midtroposphere to upper troposphere based on the observation that for several cases high ozone is associated with isentropic trajectories originating over the northern United States and Canada at 5 km or higher. *Savoie et al.* [1992] use back trajectories with multiple chemical tracers to demonstrate the role of transport in determining the strong anticorrelation of aerosol nitrate concentrations and ozone at the Barbados AEROCE site. They conclude that elevated ozone is associated with transport from higher latitudes over North America and the North Atlantic and high $NO_3^-$ is associated with transport from Europe and North Africa. These analyses demonstrate that trajectories can be useful in case studies to explain the processes influencing chemical variability.

Taking all trajectories together, however, we have quantified seasonal and interannual differences in the large-scale motion that ultimately influence variability in the concentrations of ozone and other tropospheric chemical tracers. We used the AEROCE trajectory data in this ensemble mode and objectively determined flow

[1]Department of Environmental Sciences, University of Virginia, Charlottesville.
[2]National Oceanic and Atmospheric Administration, CMDL, Boulder, Colorado.
[3]National Oceanic and Atmospheric Administration, GFDL, Princeton University, Princeton, New Jersey.
[4]Graduate School of Oceanography, University of Rhode Island, Narragansett.

climatologies by season for the Bermuda receptor. These flow climatologies characterize patterns in the large-scale motion which indicate that different source regions dominated at different times of the year. We used the multivariate method of cluster analysis to identify groups of days within each season with similar back trajectories and therefore relatively similar air-mass origin. If the chemical composition of an air parcel is influenced by its transport path, then grouping air parcels on the basis of similar back trajectories should explain a significant portion of the variability in observed chemistry. *Moody* [1986] first developed this application of cluster analysis as a pattern recognition technique for atmospheric transport. Since then, it has been used to characterize precipitation composition at several locations, both in the remote areas (*Moody and Galloway* [1988] Bermuda, and *Moody et al.* [1991], Amsterdam Island) and in the source region (*Moody and Samson* [1989], Midwestern United States, and *Dorling et al.* [1992], Scotland). Most recently this method was used to explain the seasonal variability in methane concentrations at Mauna Loa [*Harris et al.*, 1992].

## Data

### Ozone

Ozone was measured using a commercially built $O_3$ monitor manufactured by Dasibi Environmental Corporation. Over the course of the measurements discussed, two Model 1003-AH instruments with concurrent internal temperature and pressure data were used. The monitor uses the absorption of ultraviolet radiation by $O_3$ at 254 nm as the principle of measurement. The $O_3$ zero and gain of the instrument were checked every three days with an $O_3$ zero source and a fixed concentration of $O_3$. Calibration of the monitor was done by intercomparison with the Boulder, Colorado, based NOAA Climate Monitoring and Diagnostics Laboratory (CMDL) network standard ozone monitor. This standard ozone monitor was in turn compared, approximately biennially, with the standard photometer maintained by the U.S. National Institute of Standards and Technology. The $O_3$ monitors in Bermuda were intercompared in July 1988, January 1990, November 1990, and August 1991. The precision of hourly average measurements used here was plus or minus 2 ppbv or better and the accuracy based on the intercomparison technique was also plus or minus 2 ppbv [*Oltmans*, 1981].

Air at the site was sampled from the top of the 20-m AEROCE tower, the base of which is 30 m above the ocean surface. The small line losses from the nonreactive intake line running from the top to the base of the tower were corrected for by calibrating the instrument both with and without the line in place. The 20-sec samples were averaged to produce hourly means. The ozone data merged with trajectories in the following analyses represent 12-hour average values, calculated from 6 hours before through 6 hours after each trajectory time (0000 and 1200 UTC, respectively).

For the analyses reported here, all recorded hourly average $O_3$ data were used. To the east of the sampling site there is a U.S. naval facility and a road. When the wind was from this direction, there was an occasional, noticeable influence on the measurements, giving depleted ozone amounts. The wind sector under which such influences occurred was much smaller than the out-of-sector winds designated for aerosol sampling. From an examination of all of the hourly $O_3$ data, we determined that 5% or less were influenced by these nearby sources.

### Isentropic Trajectories

An atmospheric trajectory is the modeled pathway of a hypothetical parcel of air advected by a designated wind field backward or forward in time from a selected site. Over populated continental regions, upper air observations are available at high spatial and temporal resolution; the required objective analysis of wind and temperature fields can proceed directly from the sounding data. However, with long-range transport over the open ocean, model-gridded wind and temperature fields must be used as the meteorological basis for trajectories [*Merrill et al.*, 1989]. The global "analysis" of the National Meteorological Center (NMC) is a gridded set of meteorological fields, the product of a sophisticated data assimilation, initialization, and forecasting system. Its salient characteristics are modest spatial (2.5° of latitude by longitude) and temporal (12-hour interval) resolutions. We interpolated the NMC-gridded winds to potential temperature surfaces using the technique described by *Merrill et al.* [1986]. The interpolated wind fields on these isentropic surfaces were used to make the trajectory calculations.

In isentropic trajectory analysis the three-dimensional adiabatic motion of the air is accounted for even though such subgrid-scale phenomena as convection and turbulent mixing are not resolved [*Danielsen*, 1961; *Merrill et al.*, 1989]. Although routinely available meteorological data do not include vertical velocity information, the imposed constraint of motion along a potential temperature surface implicitly determines the adiabatic vertical motion. Isentropic transport assumes air parcels move about free of diabatic effects such as mixing of mass or internal energy, phase changes of water, or radiative divergence. This approximation is reasonably well satisfied at large scales of motion in the free troposphere, i.e., above the surface mixed layer and for periods of a few days. However, in regions of widespread cloudiness and precipitation and in more limited regions of strong mixing (areas of exceptionally strong wind shear, for example), the approximation breaks down. Either diabatic motions, which cross potential temperature surfaces, or multivalued potential temperatures may spoil the analysis. The approach used here differs in detail but not in principle from that used in the package described by *Haagenson and Shapiro* [1979].

For the AEROCE program we routinely calculate two trajectories per day (at 0000 and 1200 UTC), at a number of different potential temperature levels (295, 300, and 305 K). In this study we have chosen one trajectory to represent each 12-hour time period. We scanned all available potential temperature levels and selected the one which not only arrived closest to the boundary layer but also extended back at least two days. When a deep mixed layer was resolved by the large-scale analysis, the selected potential temperature surface could have repre-

sented transport at elevations above 1.5 km. That is, we did not take account of transport in the boundary layer, and additionally, upward motion approaching the site was discounted by this selection. This treatment is adequate when subsidence and surface divergence limit the transport time within the boundary layer. Under other conditions, for example when the flow is confined to the boundary layer around the subtropical high, the vertical shear of the wind is smaller than it is in strongly baroclinic situations, reducing the severity of the approximation. *Pickering et al.* [1994] suggest a lack of confidence in isentropic trajectory analysis based on differences in trajectories calculated from NMC and ECMWF fields. The measure of difference used is the distance between end points of trajectories at points along the path. Trajectories passing separately over broadly similar source areas may be marked significantly differently in such an analysis. Further, the *Pickering et al.* (1994) study is over the South Atlantic, and the distribution of upper air stations over the adjoining continents is less dense than for the North Atlantic.

We have summarized the limitations of model calculations here to temper any tendency to overinterpret information provided by trajectories, and we do not suggest that the details of each trajectory accurately reflect the actual path of motion of a reactive chemical substance like ozone. However, we do propose that this ensemble mode of trajectory analysis provides a useful representation of the relative patterns of large-scale atmospheric motion. Implicit in this approach is the expectation that relevant transport processes are influenced by large-scale atmospheric motion. *Haagenson and Sperry* [1989] show that there is a reasonable association of synoptic type with mean transport direction for an ensemble of trajectories. This strengthens our hypothesis that events with similar back trajectories may also have undergone similar transport and air-mass evolution.

## Method

We reduced the overall variability in both the large-scale atmospheric flow and the associated source regions these flows represent, by using cluster analysis to group the back-trajectory data into (n) distinct groups. Our clustering technique was a hybrid, hierarchical/iterative scheme based on a Euclidean measure of similarity with the initial hierarchical analysis designed to minimize within-group variance [*Moody et al.*, 1991]. We used the hierarchical Ward's method [*Romesburg*, 1984] to identify the number of patterns (n) and then used an iterative routine to optimize the grouping into the n clusters. Our specific approach was to plot the rate of change of the increase in within-group variance as the trajectories were grouped together (effectively, the second derivative of Ward's coefficient). We clustered the data by calendar quarter; in each cluster analysis there was a well-defined inflection point in this measure which signaled the union of two trajectory groups which were significantly more different than any trajectories combined up to that point. This designated the number (n) of patterns in the data. We then used an iterative cluster routine to optimize the n-cluster solution, overcoming the limitation of a hierarchical cluster method.

It is important to emphasize that this approach (cluster analysis) did not impose a classification structure onto the data. Neither the types of clusters (e.g., rapidly subsiding flow from the northwest) nor their numbers (n) were specified a priori. Rather, both the number and the type of transport clusters were objectively determined, reflecting the natural, preexisting relationships and patterns among the trajectories. It is precisely these patterns in the large-scale flow field that the cluster method was designed to identify, and it did an effective job. The patterns we have observed are clearly linked to the synoptic-scale features that are known to influence Bermuda, e.g., anticyclonic motion associated with the Bermuda high, strong northwesterly flow behind a cold front or a trough, etc. In this way, by objectively grouping periods of similar isentropic motion (i.e., trajectories), we created subsets of chemical measurements that were made under similar synoptic-scale conditions evolving over several days.

Using cluster techniques we simultaneously considered several important characteristics of the motion. Our calculation was a linear optimization operating on the matrix of trajectory endpoints. Since not all trajectories extended back a full 10 days (because of missing meteorological data or because they went beyond the model domain), we used trajectory endpoints (i.e., latitude, longitude, and pressure coordinates) out to 5 days back for the clustering. Implicit in the use of these variables, we characterized similarity based on horizontal and vertical wind velocities (i.e., speed and direction) as a function of time. Using these three position variables at 12-hour intervals, 5 days upwind, we effectively performed the clustering in a 30-dimensional space. However, we had the advantage of graphically viewing the result, as one can see in the next section.

After the trajectory clusters were defined, we compared their physical and chemical characteristics using nonparametric statistics [*Conover*, 1980]. We used the Kruskal-Wallis test (a conservative statistic that does not assume Gaussian distributions) to identify significant differences in the meteorological variables and $O_3$ concentration distributions between the clusters. Once the statistically significant differences in composition were established, we then estimated the ozone variance explained by the differences in transport using a standard parametric analysis of variance. Once we had partitioned the data into subgroups (trajectory clusters, or seasons), an analysis of variance (ANOVA) was used to determine if the differences in mean ozone were what might be expected from chance or random variation, or if in fact there was also a systematic variation attributed to the partitions made in the data. An ANOVA assumes that whatever differences existed between the ozone averages for each transport pattern could be attributed to two important components: (1) variability in ozone *between* the transport patterns, measuring both systematic and random variation [*Walpole and Myers*, 1978], and (2) variability *within* the transport patterns, measuring only random variation. Although the Kruskal-Wallis test indicated that there was statistically significant systematic variation among ozone subgroups (e.g., transport cluster or season), the ANOVA provided a quantitative estimate of how much of the variability was explained by the partition.
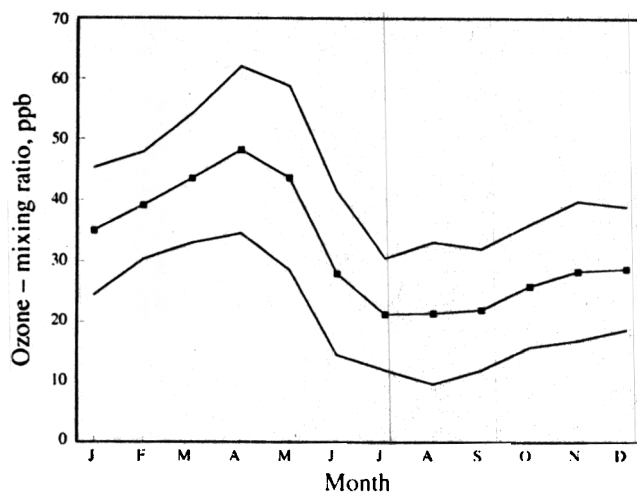
## Results

### Seasonal Variations in Ozone and Large-Scale Atmospheric Motion

The $O_3$ averaged by month showed a peak in April and a distinct minimum during the summer months of July, August, and September (Figure 1). *Oltmans and Levy* [1992] discuss this seasonal cycle and attribute the April peak to the transport of ozone from the lower stratosphere and the low summer values to clean marine air that undergoes photochemical destruction of ozone. They made this analysis based on a visual inspection of the transport data. We have quantified their observations and extended them to a larger number of cases.

As a start we simply mapped the ensemble of all trajectories for each season. Using all the trajectories for each quarter of the year (e.g., January-March), we plotted the probability density function describing the relative likelihood of air parcels arriving from any upwind region. Several papers present trajectories similarly [*Samson and Moody*, 1981; *Poirot and Wishinsky*, 1986; *Merrill and Graustein*, 1989]. We described each trajectory end point as the center of a Gaussian puff using the method of *Samson and Moody* [1981]. We then summed the probability fields for each individual trajectory to represent the ensemble probability, or pattern, for a given set of trajectories.

The overall patterns of large-scale atmospheric motion corresponding to four quarters on Bermuda (January-March, April-June, July-September, and October-December, which for simplicity we also refer to as winter, spring, summer, and fall) are given in Plate 1. Each panel summarizes 540 trajectories a quarter (2 trajectories a day for 3 years). The average pressure 5 days back along the trajectories and the 12-hour-average $O_3$ concentration measured on Bermuda appear in each panel. The Bermuda high dominated transport during the summer months, July through September, when $O_3$ was lowest. There was a high probability of transport from the south and east and a correspondingly low average $O_3$ of 22

ppbv. By contrast, during the months of April through June, the probability of subsiding air from the north (average pressure 5 days back of 800 hPa) was enhanced and the average $O_3$ was much higher. This is shown by the region of high probability that extends back over the northern Midwest and Canada. A comparison of the average pressure profiles for these different seasons indicates that the air was more likely to come from higher elevations 5 days back during the spring than during the summer. The transport probabilities for winter (January-March) and fall (October-December) resemble those for spring (April-June) except that they were associated with a slightly more zonal (west-to-east) wind pattern. The quarter-average $O_3$ values for fall and winter were similar to spring; however, standard deviations were lower, indicating less variability. The extreme concentrations of $O_3$, in the 60- to 80-ppbv range, were only seen in the spring.
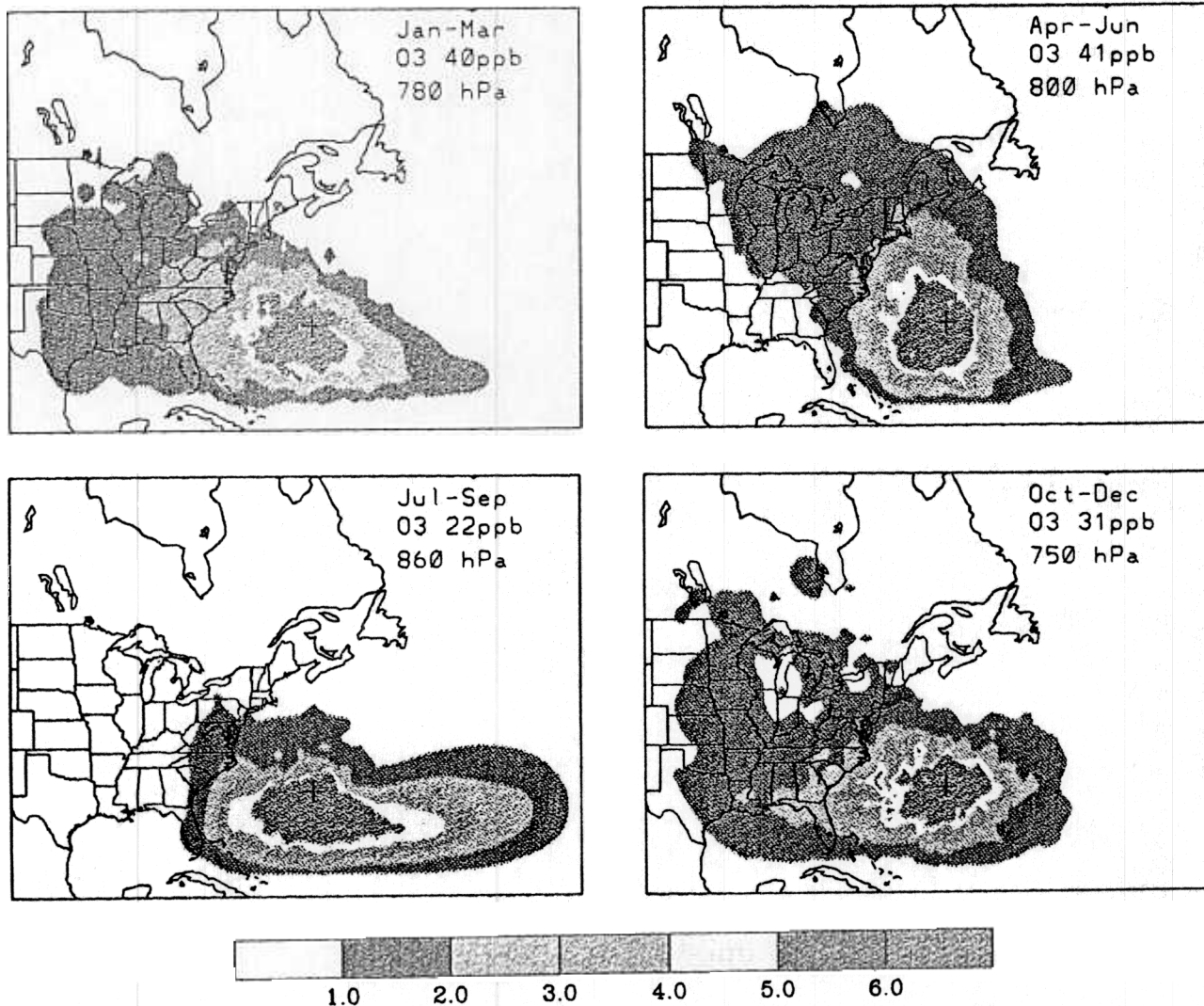
These results give the impression that variability in ozone was driven, to a significant degree, by differences in transport. We sought to quantify this relationship by looking at the variability within a season. Our focus was on April-June, the spring quarter when the $O_3$ concentrations over Bermuda were the highest.

### Cluster Analysis of Back Trajectories

A cluster analysis of 540 back trajectories was run using April through June data from 1989 through 1991. We had to exclude 100 trajectories because they did not go back a full 5 days. These represent a mixture of times with no trajectory (as a result of missing meteorological data) or times when the trajectories terminated in less than 5 days, either because of missing meteorological data or because trajectories ran off the grid they were calculated on or the potential temperature they represented ran into the surface of the Earth. These 100 events, with all these reasons combined, had an average $O_3$ concentration of 38 ppbv, slightly less than the spring average of 41 ppbv.

The hierarchical/iterative cluster analysis scheme identified seven distinct transport patterns in the 440 5-day back trajectories. To illustrate how effective the cluster analysis was, we have plotted three of the resulting groups (Figure 2). These trajectory ensembles represent transport patterns of low-level anticyclonic flow from the south and east around the Bermuda high (Figure 2a), relatively low wind-speed flow from the southwest (Figure 2b), and high speed flow off the North American continent descending to Bermuda from relatively high levels (Figure 2b).

The trajectories within each group were characterized by relatively similar wind direction, wind speed, and atmospheric pressure (the measure of vertical motion), further corroborating that these periods shared a similar transport history. We calculated probability fields (similar to those shown in Plate 1) to summarize the potential contribution of transport from upwind regions for each pattern. Plate 2 shows these same three clusters as probability fields, along with the average pressure profile and the ozone frequency distribution. The pressure profiles illustrate the vertical motion associated with the transport as a function of 2-hour time steps back along the trajectory. Under meteorological conditions where



**Figure 1.** Average ozone concentration by month for Bermuda, 1989-1991. The arithmetic mean (solid squares) and plus and minus one standard deviation are plotted [adapted from *Oltmans and Levy*, 1992].

Plate 1. Patterns of large-scale atmospheric motion influencing the Bermuda site. The four quarters of the year are represented with probability fields describing the relative likelihood of air parcels arriving from upwind regions. In addition to representing the probable airflow for each quarter, the 12-hour average ozone concentration and the average pressure 5 days back along the trajectories have been included.

there was very little thermal stratification indicative of a deep mixed layer, the initial pressure of the back trajectory could have been as high as 700 mbar (~3 km). As a result of this, we found that the clusters showed different initial pressures at Bermuda depending on the thermal structure of the boundary layer.

For each of these transport patterns, there were well-defined differences in the site meteorological data (temperature, water vapor mixing ratio, atmospheric pressure, wind speed, and precipitation amount) collected on the Bermuda tower, which further corroborated that clustering trajectories into periods of similar large-scale motion effectively distinguished different air masses. Now we will illustrate that these air masses delivered significantly different amounts of $O_3$.

The three distinct patterns in Plate 2 illustrate transport around the Bermuda high (BH), transport from the southwest (SW), and transport from the northwest (NW), respectively. The most striking result was the strong

association of elevated ozone with NW subsidence. In particular, when we compared the results in Plate 2a to those in Plate 2c, the ozone distributions only barely overlapped. Under northwesterly flow, the $O_3$ concentrations were uniformly greater than 40 ppbv with rapid subsidence from the continental interior (Figure 2c). In contrast, flow around the Bermuda high rarely exhibited $O_3$ values over 40 ppbv (Figure 2a). The pattern of flow from the SW delivered significantly more precipitation than any of the other clusters. Consistent with this observation, the pressure profile exhibits rising motion within the last 2 days of transport. Note that the initial pressure for these events shows an average starting pressure of 850 mbar (~ 1.5 km). These trajectories were the ones that started closest to the boundary layer and still extended back far enough to be included in the clustering (at least 5 days). Although there may have been another trajectory with a lower potential temperature that started closer to the boundary layer, it would
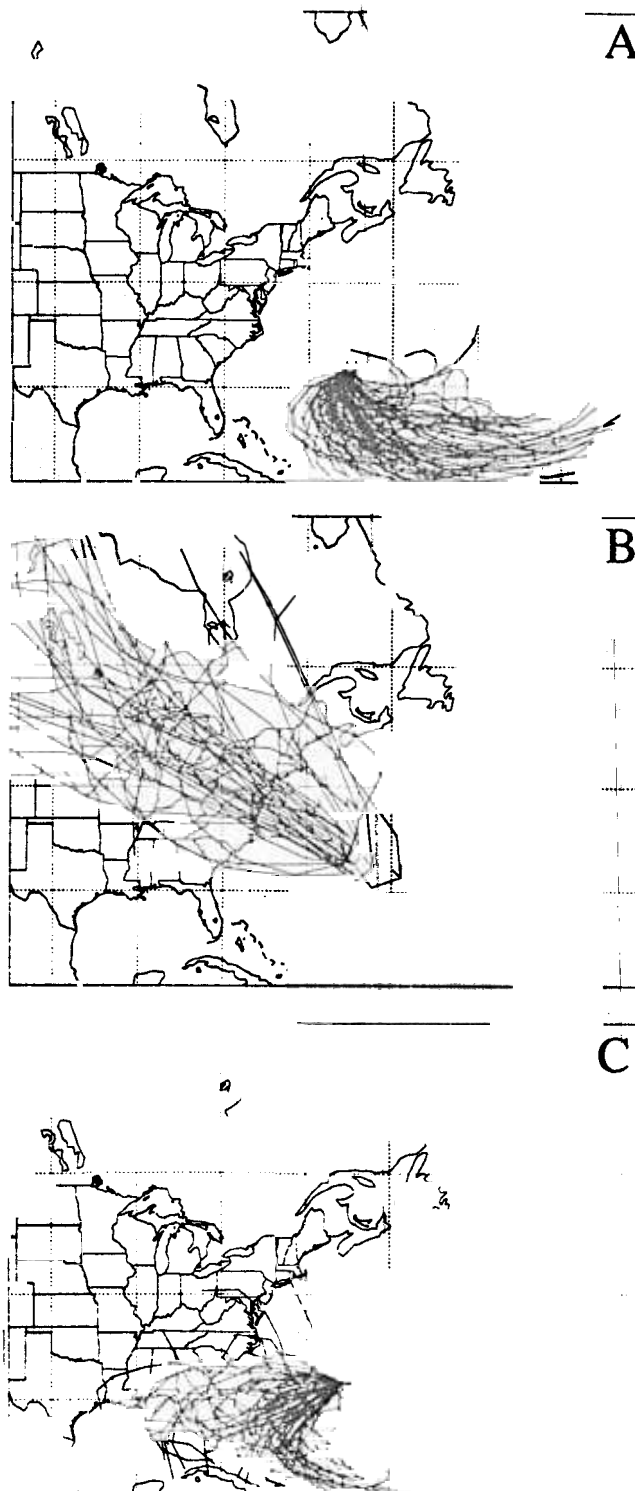
Figure 2. Three of the seven spring quarter (April-June, 1989-1991) trajectory clusters identified in the data: (a) Anticyclonic flow around the Bermuda high, (b) flow from the southwest at relatively low speed, and (c) high-speed flow of North American continental origin.

have likely intersected the surface within a short distance back, given these conditions of rising motion.

Of the seven cluster patterns identified in the spring trajectories, four clusters (not shown) shared a flow from the continent; however they were classified as different groups on the basis of wind speed or vertical motion (i.e., pressure profile). For example, there was a pattern with flow from the northwest that resembles the category NW subsiding but had much slower subsidence and lower wind speeds between the United States eastern coast and Bermuda. These conditions sometimes delivered elevated ozone concentrations but not as consistently as the rapidly subsiding transport shown in Plate 2c. When we considered all the trajectories that originated over the continent, we found these conditions prevailed 41% of the time but they encompassed 91% of all the 12-hour periods with average $O_3$ values greater than 60 ppbv.

Figure 3 presents the deviation of mean $O_3$ in each of the seven transport patterns from the seasonal mean for the spring of 41.4 ppbv. Ozone was significantly enhanced in the west (US) and northwest continental flow, in general, and in the rapidly subsiding NW flow, in particular. We have evaluated these differences in a number of ways. First we used nonparametric statistics to test the hypothesis that the distributions all had the same mean concentration. This hypothesis was rejected with 99% confidence. Having determined this systematic variation was statistically significant, we then used a standard parametric analysis of variance to estimate the percent of ozone variability explained by the differences in transport (Table 1). We found that, in the spring clusters, over 40% of the variance in ozone could be explained simply by changes in the large-scale flow patterns represented by the seven clusters.

In similar fashion we determined the cluster patterns for the other seasons. In each quarter, well-defined differences in transport were based on the horizontal and vertical wind information characterized by trajectory endpoints. Again, we found a significant variability in ozone was explained by these differences in large-scale transport. To simplify the presentation of seasonal results in Plates 3-5 (July-September, October-December, and January-March, respectively), we have included only the clusters representing the three distinct patterns: (1) transport around the Bermuda high (BH); (2) transport from the southwest (SW); and (3) the rapidly subsiding flow from the northwest (NW$_{sub}$). We have also shown the deviation of mean $O_3$ in these three transport patterns from the overall mean for each quarter (January-March, July-September, and October-December, respectively, Figure 4). In each season, the lowest $O_3$ concentrations were transported from the open ocean in flow around high-pressure systems. The lowest concentrations of $O_3$ in BH flow conditions occur in the summer quarter (July-September). When transport was from the southwest with a likely contribution of some continental air from the southern United States, the ozone concentrations were somewhat higher. But, in each season, meteorological conditions associated with the rapidly subsiding transport from the midtroposphere northwest of Bermuda delivered the highest concentrations of $O_3$ (see Figure 5 and Plate 2c).

We used the analysis-of-variance technique to characterize how much of the ozone variability for one transport pattern (e.g., BH) was explained by seasonal differences and how much of the variability in one season (e.g., spring) was explained by transport differences, considering only the three main patterns of transport. The results are presented in Figure 5. In the winter (January-March) we
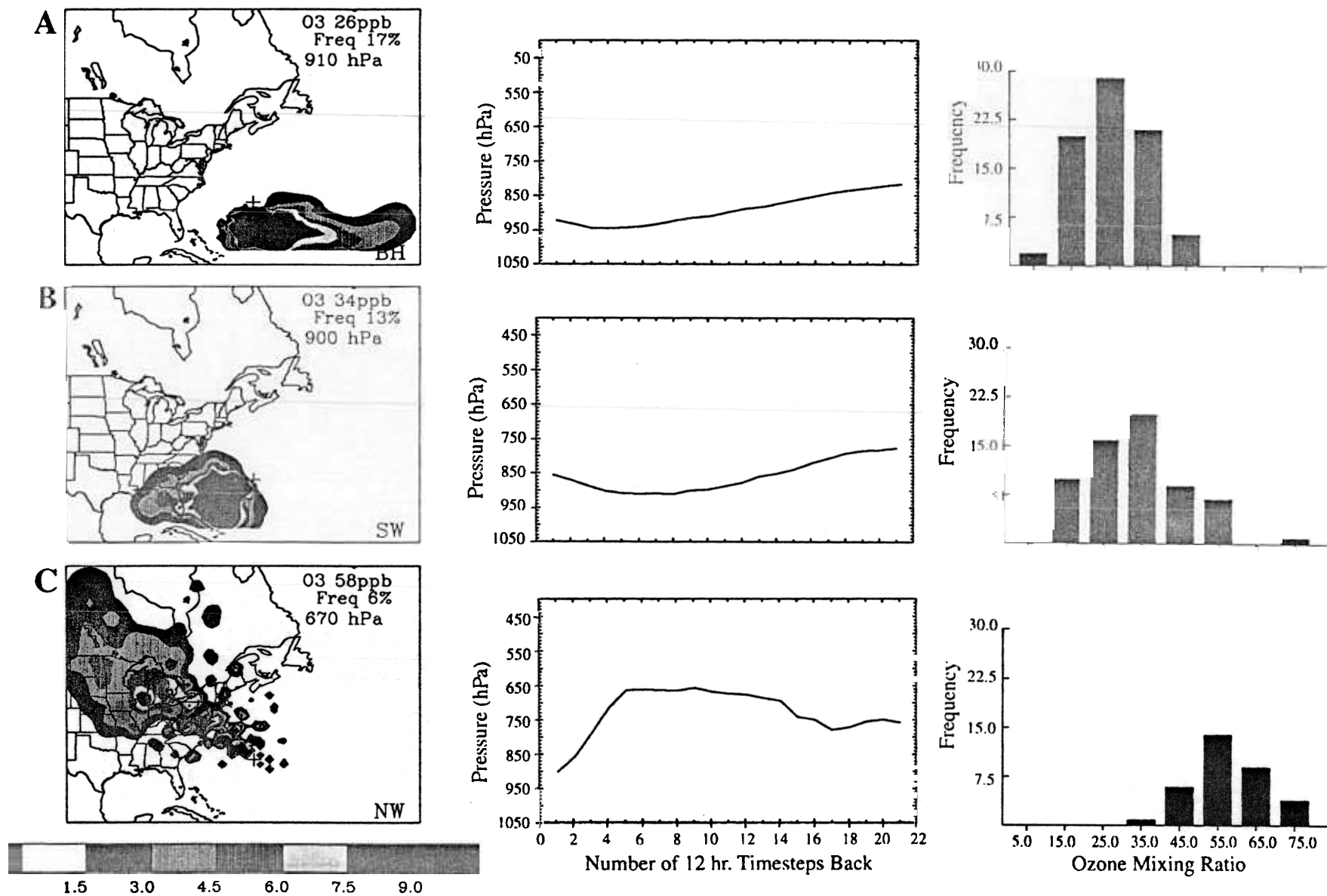
**Plate 2.** Three of the seven clusters derived for the spring period presented as probability fields. These describe the relative likelihood of air parcels arriving from upwind regions. (The same scale of probability presented in Plate 1 applies here, with potential contribution increasing from cool to hot colors.) Along with transport fields a profile of average pressure along the trajectory and the ozone concentration frequency distribution are presented for (a) anticyclonic flow around the Bermuda high (BH), (b) rising motion from the southwest at relatively low speed (SW), and (c) high-speed subsident flow of North American continental origin (NW-subsiding).
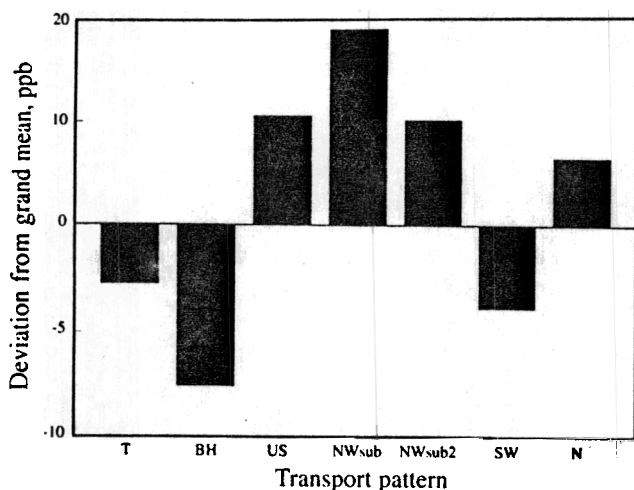
**Figure 3.** Deviation of mean ozone in each of the seven spring quarter (April-June) transport patterns from the grand mean for the season of 41.4 ppb. "T" represents transitional flow patterns.

found that only 30% of the variability in $O_3$ could be explained by differences in large-scale transport, indicating that there was significant residual variation within each of the transport patterns. The largest seasonal variability occurred in April through June ($\sigma^2 = 266$) and we found that transport differences between the three main patterns explained 55% of this variation. In summer and fall, 37% and 33%, respectively, of the within-season variability in ozone was explained by differences in large-scale transport.

Looking between seasons at the variability within a given transport pattern, we identified that flow around the Bermuda high was least variable ($\sigma^2 = 92$) and 50% of the variation could be explained by seasonal differences, with the lowest $O_3$ concentration in the summer quarter and the highest BH $O_3$ in the winter. This is consistent with the $O_3$ associated with this pattern being controlled by photochemical destruction and surface loss, with both being greatest in the summer.

$O_3$ varied much more when only flow from the NW ($\sigma^2 = 132$) or flow from the SW ($\sigma^2 = 149$) was considered. In SW flow, seasonal differences only accounted for 26% of the variance in ozone concentrations. This pattern encompassed both oceanic and continental sources, which could explain the large residual variability within this

cluster. For NW flow, 58% of the variability was explained by seasonal variations. This illustrates that, although large-scale motion resulting in NW subsidence occurred throughout the year, there were significant seasonal differences in $O_3$ even under these flow conditions. This is a significant and important result. It tells us that, even under the specific conditions of subsiding flow from the NW, there exists a seasonally varying source or atmospheric process that results in highest ozone in the spring months.

A synoptic analysis of the spring events in 1989-1991 associated with strong subsidence under NW flow shows that they are clearly indicative of the transport behind cold fronts which have just penetrated to Bermuda. The local site meteorology shows the temperature drops, the air drys out, the pressure rises, and the surface winds become northerly. The fronts themselves are well-defined and easily detected on weather maps and in satellite images. An analysis of the upper level meteorology leading up to these events shows deepening troughs or cutoff lows in the region of the back trajectories when they are at midtropospheric heights over the continent.

Spring is also the period of maximum transport of ozone from the upper troposphere and lower stratosphere and maximum levels of ozone in the midtroposphere over northern North America [Danielsen, 1968; Danielsen and Mohnen, 1977; Logan, 1985]. If the air masses delivering elevated surface $O_3$ on Bermuda in the spring were indeed originating at midtropospheric levels as suggested by the trajectories, there should be a strong anticorrelation of ozone with water vapor mixing ratio ($H_2O_v$) [Thompson et al., 1990]. In fact, for most of the year, the high concentrations of $O_3$ were associated with incursions of relatively low $H_2O_v$ mixing ratios, i.e., dry air (Figure 6). The maximum correlation between $O_3$ and $H_2O_v$ was in the spring with $r^2$ values of 0.5 and 0.7; this relationship did not hold in the summer. We also found there was significant interannual variability in this measure of downward mixing. In association with dry air, concentrations of [7]Be, a stratospheric and upper tropospheric tracer, should be elevated in the subsiding air and positively correlated with ozone [Kritz et al., 1991]. The highest April-June concentrations of [7]Be were in the NW-subsiding cluster (5.7 mBq m$^{-3}$) with the lowest value (3.6 mBq m$^{-3}$) in the BH low-level, maritime transport cluster. These observations are consistent with a contribution of natural ozone from the stratosphere. This relationship was not well characterized by a simple linear fit. We

**Table 1.** Mean of 12-hour Average Ozone Data by Quarter and Results of an Analysis of Variance Attributable to Differences in Large-scale Transport Within Each Quarter

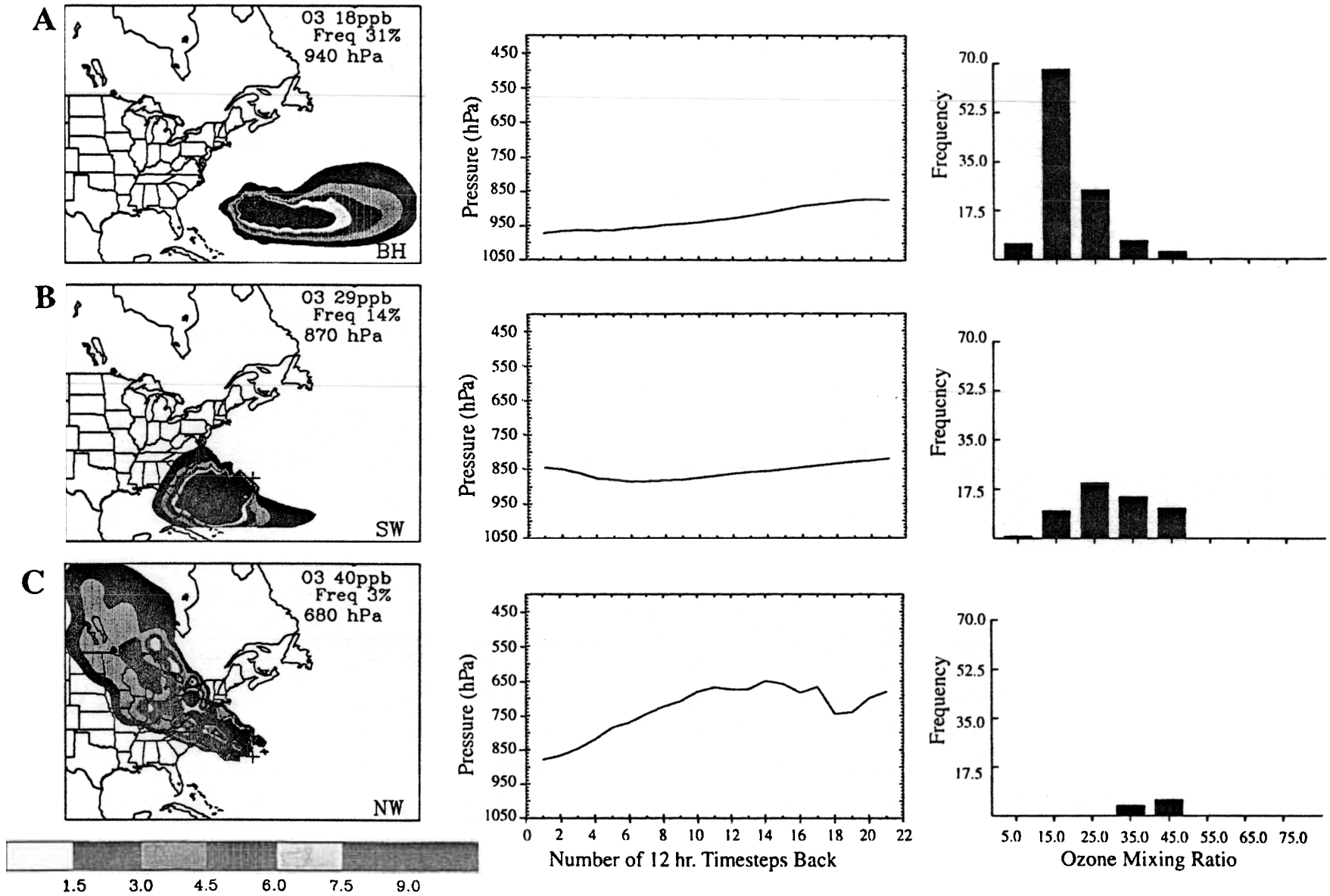|  | Mean $O_3$ $\mu$, ppbv | s.d. $\sigma$, ppbv | Variance $\sigma^2$ | Correlation With Transport | Variance Explained, % |
|---|---|---|---|---|---|
| Jan.-March | 39 | 10.4 | 108 | 0.51 | 26 |
| April-June | 41 | 16.0 | 257 | 0.65 | 43 |
| July-Sept. | 23 | 10.5 | 111 | 0.52 | 28 |
| Oct.-Dec. | 31 | 11.0 | 121 | 0.52 | 27 |

**Plate 3.** Third-quarter (July-September) clusters representing three distinct patterns: (a) Transport around the Bermuda high, (b) transport from the southwest, and (c) subsiding flow from the northwest.
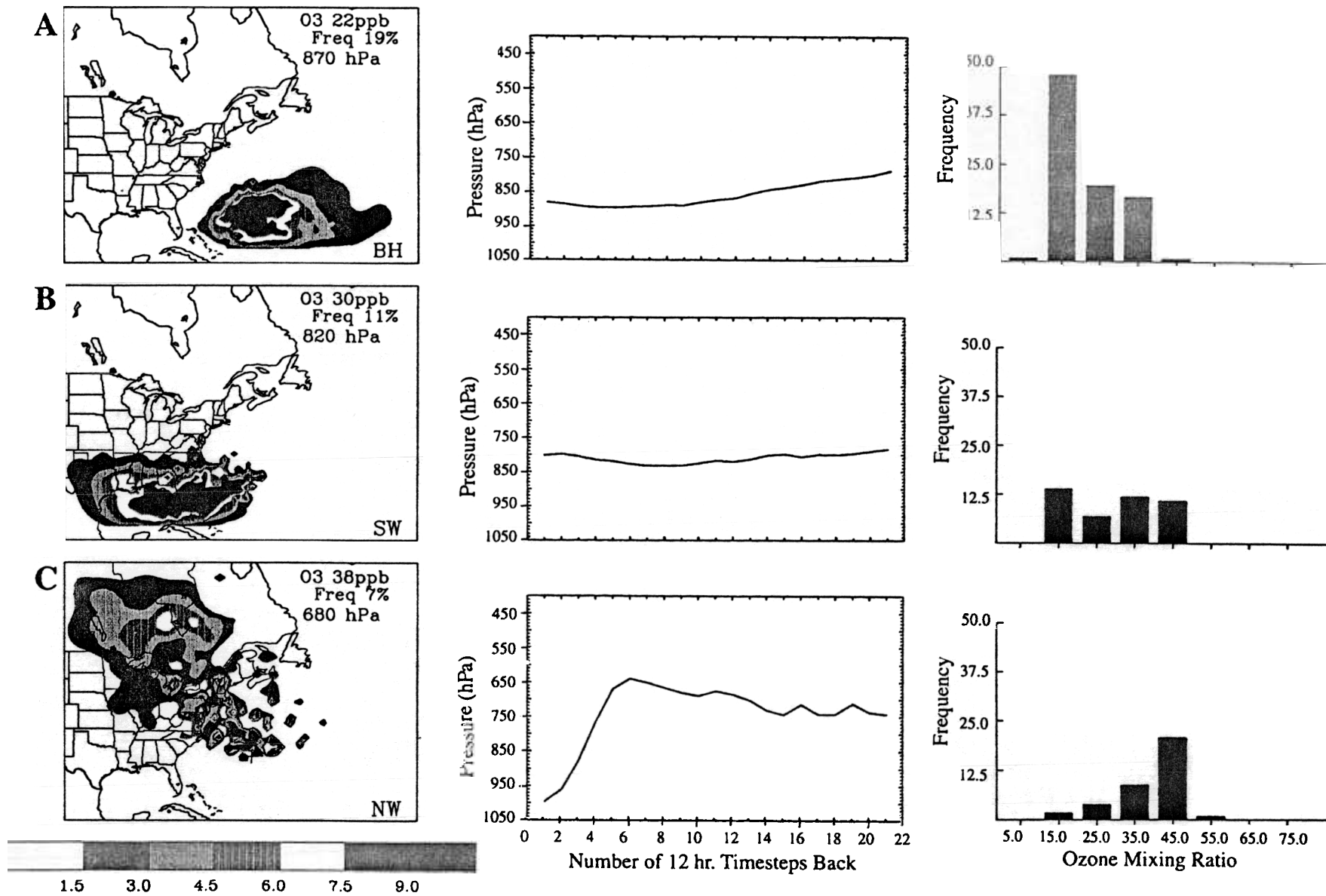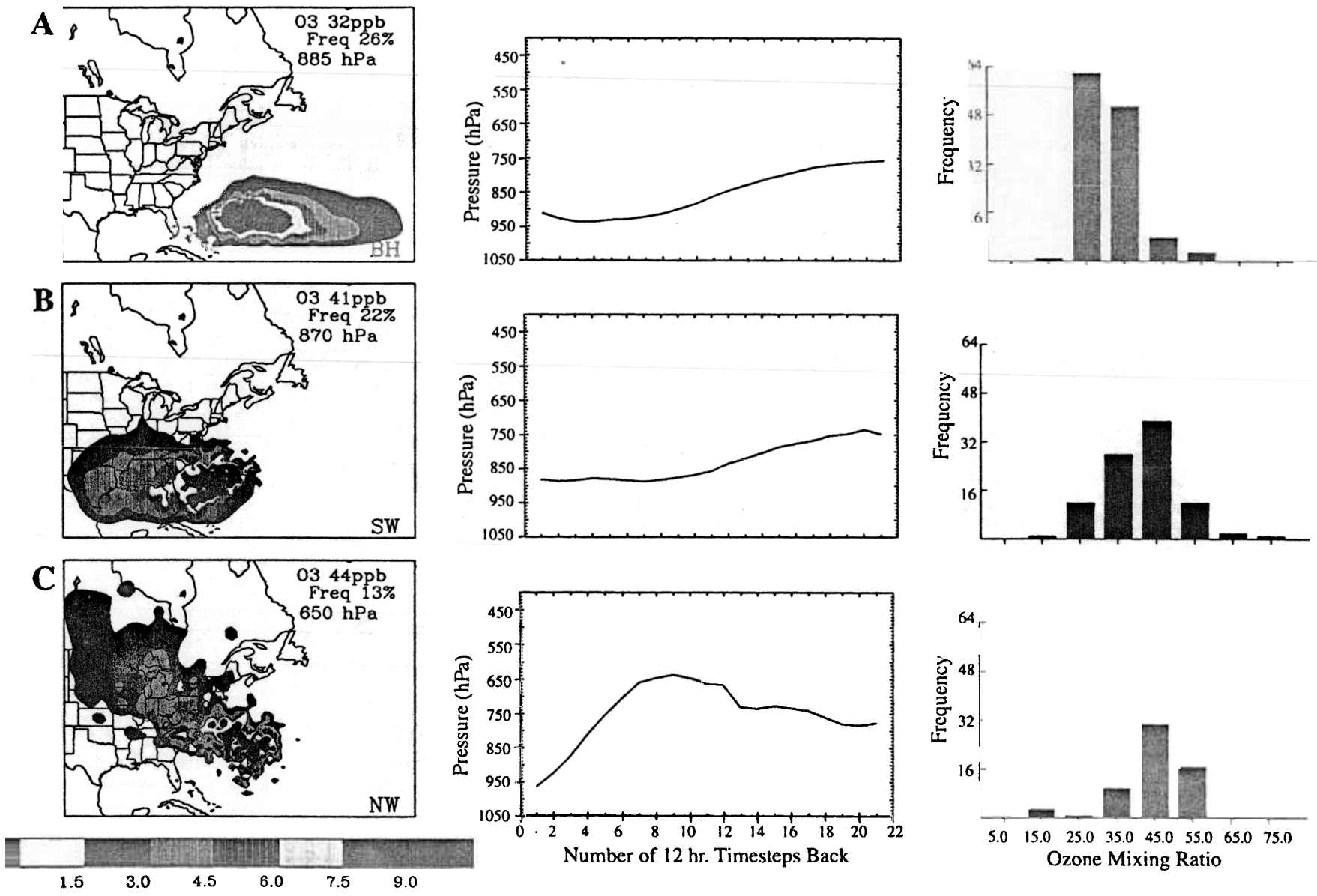
**Plate 4.** Fourth-quarter (October-December) clusters representing three distinct patterns: (a) Transport around the Bermuda high, (b) transport from the southwest, and (c) subsiding flow from the northwest.

**Plate 5.** First-quarter (January-March) clusters representing three distinct patterns: (a) Transport around the Bermuda high, (b) transport from the southwest, and (c) subsiding flow from the northwest.
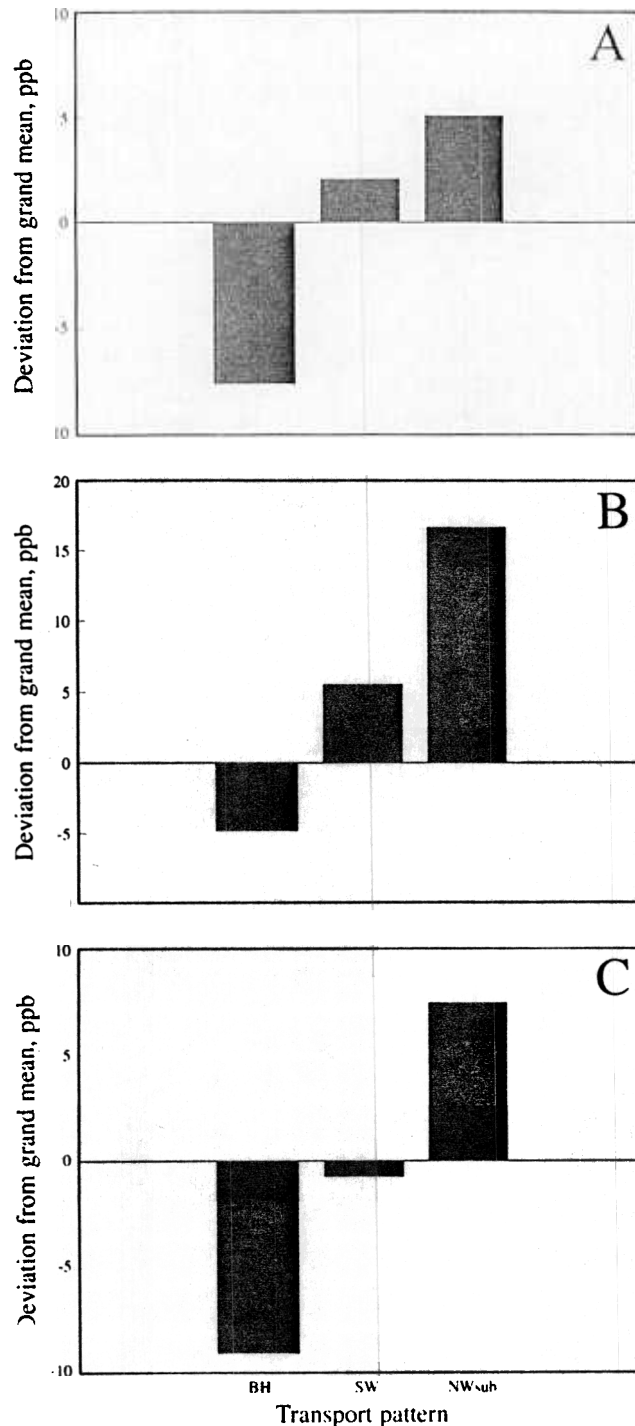
**Figure 4.** Deviation of mean ozone in each transport pattern from the grand mean. (a) 39.2 ppb for January-March, (b) 23.0 ppb for July-September, and (c) 27.4 ppb for October-December.

found $O_3$ versus [7]Be had a correlation coefficient of r=0.70 for the month of April but a correlation coefficient of r=0.34 for the entire spring (April-June) quarter. However, the data correspondence is less than ideal for deriving a correlation since the [7]Be is measured on aerosols which are subject to scavenging, and they represent a 24-hour integrated sample.

In addition to ozone and [7]Be we have estimated the concentrations of several other aerosol chemical tracers as a function of transport pattern. However, analyzing aerosol data using the cluster approach was difficult because, again, the measurements integrated as much as 24 hours of pumping, and sampling was not always continuous. On the basis of this less thorough analysis (relative to $O_3$), we found many aerosol species with continental surface sources (nss-$SO_4^=$, $NO_3^-$, Sb) were also lowest under the BH flow pattern and relatively high in the NW-subsiding cluster. There were insufficient data to do a full analysis of variance, since only a subset of all the $O_3$/trajectory periods we have analyzed had aerosol data available. However, it does appear that in the spring for example, while there were above average nss-$SO_4^=$ concentrations in the NW-subsiding cluster, the mean nss-$SO_4^=$ by cluster was higher in the other patterns that delivered air from the NW moving more slowly and subsiding less rapidly. Overall, this implies that the air masses reaching Bermuda from the NW contained air mixed in from the continental boundary layer. This does suggest two other possible sources of the elevated levels of ozone in the NW-subsiding cluster: (1) the transport of elevated ozone produced in the polluted continental boundary layer or (2) the formation of elevated levels of ozone in the free troposphere via photochemical ozone production during transit. In the next section we will discuss the climatological results we have presented in this paper in light of previous work which has evaluated the various sources of tropospheric ozone.

## Discussion

Studies that have measured the stratosphere/ troposphere exchange process using radioactive and meteorological tracers and ozone and aerosol backscatter from airborne and surface-based lidar [Ancellet et al., 1991; Browell et al., 1987; Danielsen et al., 1987] have established a strong correlation between ozone entrained in the troposphere under conditions of high isentropic potential vorticity and attendant mixing [Ancellet, 1994; Appenzeller and Davies, 1992; Shapiro, 1980]. This flux is episodic in nature and is associated with baroclinic instability; it occurs as air is extruded from the lower stratosphere on the poleward side of the jet stream during large-scale cyclogenesis. These conditions often precede the passage of strong midlatitude synoptic systems along the eastern coast of the United States, with the cold front often penetrating Bermuda as the storms occlude over the maritime provinces of Canada. Their frequency is at a maximum during the spring months.

These meteorological conditions are similar to those presented in an analysis of the relationship between elevated surface ozone and ozonesonde profiles and their association with spring cold frontal systems over Japan [Wakamatsu et al., 1989]. On the basis of intensive observations it was concluded that high surface ozone in the spring (occurring with high pressure and dry air) is ultimately delivered from the upper troposphere after stratospheric intrusions. Preceding this study by several years, Chatfield and Harrison [1977] showed a meridional variation in tropospheric ozone (from sondes) with a ridge of ozone greater than 60 ppbv in the 3- to 7-km region

| Season | $O_3$ Transport Patterns, ppbv | | | Variance Within Quarter | Variance Explained by Transport Differences, % |
|---|---|---|---|---|---|
| | BH | SW | $NW_{sub}$ | | |
| Jan.-March | 32 | 41 | 44 | 102 | 30 |
| April-June | 26 | 34 | 58 | 266 | 55 |
| July-Sept. | 18 | 29 | 40 | 109 | 37 |
| Oct.-Dec. | 22 | 30 | 38 | 87 | 33 |
| Variance within transport patterns | 92 | 149 | 132 | | |
| Variance explained by seasonal (quarter) differences | 50% | 26% | 58% | | |

Figure 5. Mean 12-hour average ozone data by quarter and transport pattern with a summary of the analysis of variance showing differences in transport by season and differences between seasons for a given transport pattern. BH, transport around the Bermuda high; SW, transport from the southwest; $NW_{sub}$, rapidly subsiding transport from the northwest.

over the eastern United States. This ridge corresponds to the region of cyclogenesis over the eastern United States. They infer the influence of stratospheric $O_3$; however, they also note that their observations do not preclude a contribution of $O_3$ formation from anthropogenic precursors over eastern source regions.

Data on the concentration of $O_3$ in the spring over rural locations in the eastern United States show that there are episodes when surface $O_3$ is greater than 70 ppb over large regions [Logan, 1989]. With the exception of one event which is characterized as a stratospheric intrusion, these are attributed to photochemical production of $O_3$. However, upon reviewing the surface maps associated with other events which occurred in early spring (March and May of 1978 and 1979), we found that these were postfrontal conditions, with high pressure and
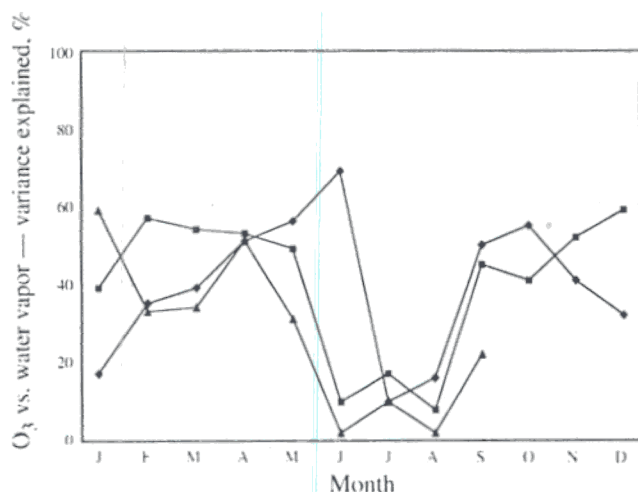


Figure 6. Percentage of variance in ozone explained by its correlation with water-vapor mixing ratio by month for 1989 (solid square), 1990 (solid diamond), and 1991 (solid triangle).

large dew point depressions, suggesting dry air at the surface with very elevated $O_3$ concentrations not unlike the synoptic conditions that lead to higher $O_3$ on Bermuda. A number of other studies have looked at tropospheric ozone data and some measure of transport (synoptic classifications, surface pressure fields) and have identified a correlation of enhanced winter and spring surface ozone concentrations with synoptic weather patterns of high pressure and strong winds, inferring from the subsidence that the ozone is of stratospheric origin [Comrie and Yarnel, 1992; Davies et al., 1992; Feister and Balzer, 1991].

Recently, in an analysis of the midtropospheric spring ozone maximum in the southern hemisphere over the South Atlantic, Krishnamurti et al. [1993] show that a complex system of horizontal and vertical transports appear to cause the $O_3$ maximum, and it appears to be influenced by stratospheric contributions. When Levy et al. [1985] modeled the global climatology of tropospheric ozone, they found that a stratospheric source, with equatorward, downward transport through the troposphere is reasonably consistent with global observations away from continental regions of pollution. A recent numerical simulation with only a stratospheric source and chemical destruction in the troposphere showed excellent agreement with the surface observations at Bermuda (H. Levy II, Geophysical Fluid Dynamics Laboratory, Princeton University, unpublished data, 1993). Alternatively, Penkett et al. [1993] propose that a potential source of the elevated free-tropospheric ozone during the spring might be in situ photochemical production from hydrocarbons that build up in the winter in the free troposphere at high latitudes and become reactive as photochemical production potential goes up after the vernal equinox. They suggest the extensive reservoir of hydrocarbons north of the polar front could be significantly influencing ozone formation in the troposphere and may be responsible for the spring peak in concentrations in the northern latitudes.

Transport from the free troposphere over North America could deliver ozone from an elevated reservoir or it could deliver relatively fresh anthropogenic air injected above the planetary boundary layer over the continental source regions in postfrontal mixing or convection that precedes these periods of subsidence [Pickering et al., 1992]. Dickerson (R. Dickerson, personal communication, 1994) suggests that this was an important mechanism in June 1992 when $O_3$ arrived on Bermuda highly correlated with CO, resulting from photochemical production within, and the dilution of, polluted air from eastern North America.   Similar behavior has been suggested in the $O_3$ data observed in the maritime provinces as part of the NARE program [Parrish et al., 1993]. Although photochemical formation during transit from $O_3$ precursors mixed up from the polluted continental boundary layer is a possibility, transport times were rapid in the NW-subsiding cluster and photochemistry would be slower than in the summer.  However, without detailed chemical calculations beyond the scope of this paper, we could not determine the amount of in-transit photochemical production of ozone.

The 1985 WATOX study looked at transport from the continent over the western North Atlantic Ocean during spring months and reported evidence of photochemical production (March and April).  One study compared $O_3$, CO, and hydrocarbon concentrations in the boundary layer and free troposphere flying offshore of Virginia and Bermuda [Van Valin and Luria, 1988]. They concluded from one flight that there was evidence of in situ production of $O_3$ in the vicinity of Bermuda.  Although this paper did not specify synoptic conditions, a separate report [Artz et al., 1986] did review meteorological conditions in detail.  Looking at these summaries along with the Van Valin and Luria data, we conclude that, similar to our results reported here, they found an increase in the free-tropospheric $O_3$ behind cold fronts both along the east coast and out over Bermuda.  This does not rule out the possibility that the elevated concentrations they saw above the boundary layer over Bermuda were associated with subsidence in the free troposphere with NW flow behind a cold front.

Before the AEROCE sites over the North Atlantic had become operational, Chatfield and Haagenson [1988] had noted that under the conditions of NW subsidence, tower instruments should effectively sample midtropospheric air.  Our climatology confirms this hypothesis.  However, there is an inherent difficulty with the Bermuda location, it lies downwind of both major anthropogenic sources and a zone which dynamically favors stratospheric injection.

Looking at the total distributions of our $O_3$ measurements, we conclude that large-scale subsidence was clearly important with strong NW winds behind cold fronts delivering dry air and the maximum ozone in each season. Moreover, even though similar large-scale transport indicating NW subsidence occurred throughout the year, it only resulted in very high $O_3$ concentrations (60- to 80-ppbv range) during the spring.  When we compared NW transport during the autumn and spring (Figure 5), our results suggested the spring midtroposphere ozone source contributed an additional 20 ppbv of ozone on the average.  This might have been contributed by a strato-

spheric source, the in situ production from pollution precursors during transport, or a contribution from both. The jump in aerosol concentrations associated with northwesterly flow on Bermuda suggests that mixing over the continent introduced anthropogenic pollutants into the air masses we have simplistically characterized as NW subsiding on the basis of the associated large-scale motion.  However, the resulting correlation of ozone with high aerosol concentrations (either anthropogenic or cosmogenic) does not necessarily reflect a common source, only a correlation on the basis of transport and mixing.

The transport patterns correlated with elevated springtime levels of ozone on Bermuda were typically associated with synoptic conditions that ventilate a surface site with free-troposphere air.  Although the ultimate source of these midlatitude, midtroposphere elevated $O_3$ concentrations remains open to discussion, evidence supports a contribution from the downward transport of stratospheric ozone.

This clearly requires further investigation. Future work will include an analysis of potential vorticity, a dynamic tracer of stratospheric air. Moving beyond the climatological view presented here, we will use this technique in a series of case study analyses for the spring months to investigate the relationship between elevated ozone concentrations and all other measurements from the Bermuda AEROCE site in an effort to better understand the meteorology and attendant chemistry on a more mechanistic level.   However, the best test of different hypotheses regarding the source of spring $O_3$ in postfrontal air will require three-dimensional profiles of both meteorological and chemical tracers carefully planned to sample air masses associated with an evolving frontal system that ultimately penetrates to Bermuda.

## Conclusions

Looking at all the available trajectory data in a systematic manner allowed us to consider events with similar histories of large-scale motion.  We identified statistically significant differences in the meteorological and chemical characteristics of the days grouped using this method.  We used the clustering technique as a large-scale meteorological filter to compare similar transport conditions at various times of the year.  Based on these results, we conclude that the AEROCE tower on Bermuda was periodically sampling midtropospheric air subsiding from the northwest in the wake of cold fronts.  These conditions were most frequent during the spring.  The large-scale motion they directly represent and whatever smaller scale exchange they might have fostered were strongly correlated with maximum surface $O_3$ concentrations observed on Bermuda.

Although the ultimate origin of these midlatitude, midtroposphere, elevated $O_3$ concentrations is still uncertain, based on the evidence of meteorological events and the dynamics of the baroclinic systems which delivered these enhanced concentrations, our results suggest a significant contribution of $O_3$ from the upper troposphere and lower stratosphere. We have acknowledged these same transport conditions also entrained polluted, conti-

nental, boundary layer air. With further analyses we expect to gain a better understanding of what fraction of this ozone might be associated with air that ultimately came from the stratosphere versus what fraction came from anthropogenic sources.

# References

Ancellet, G., M. Beekman, and A. Papayannis, Impact of a cutoff low development on downward transport of ozone in the troposphere, *J. Geophys. Res.*, *99*, 3451-3468, 1994.

Ancellet, G., J. Pelon, M. Beekmann, A. Papayannis, and G. Megie, Ground-based lidar studies of ozone exchanges between the stratosphere and the troposphere, *J. Geophys. Res.*, *96*, 22,401-22,421, 1991.

Appenzeller, C., and H. C. Davies, Structure of stratospheric intrusions into the troposphere, *Nature*, *358*, 570-572, 1992.

Artz, R. S., U. Day, and S. G. Sheridan, Meteorological summary of WATOX 1985 research intensive, February-April, *NOAA Tech. Memo., ERL ARL-145*, 76 pp., Environ. Res. Lab., Silver Spring, Md., May 1986.

Browell, E. V., E. F. Danielsen, S. Ismail, G. L. Gregory, and S. M. Beck, Tropopause fold structure determined from airborne lidar and in situ measurements, *J. Geophys. Res.*, *92*, 2112-2120, 1987.

Chatfield, R., and P. Haagenson, Sampling mid-tropospheric air at AEROCE surface sites, in *Tropospheric Ozone: Regional and Global Scale Interactions*, edited by I. S. A. Isaksen, pp. 371-380, D. Reidel, Norwell, Mass., 1988.

Chatfield, R., and H. Harrison, Tropospheric ozone, 2, Variations along a meridional band, *J. Geophys. Res.*, *82*, 5969-5976, 1977.

Comrie, A. C., and B. Yarnel, Relationships between synoptic-scale atmospheric circulation and ozone concentrations in metropolitan Pittsburgh, Pennsylvania, *Atmos. Environ.*, *26(B)*, 301-312, 1992.

Conover, W. J., *Practical Nonparametric Statistics*, 220 pp., John Wiley and Sons, New York, 1980.

Crutzen, P. J., Tropospheric ozone: An overview, in *Tropospheric Ozone Regional and Global Scale Interactions*, edited by I. S. A. Isaksen, pp. 3-32, D. Reidel, Norwell, Mass., 1987.

Danielsen, E. F., Stratospheric-tropospheric exchange based on radioactivity, ozone, and potential vorticity, *J. Atmos. Sci.*, *25*, 502-518, 1968.

Danielsen, E. F., Trajectories: Isobaric, isentropic and actual, *J. Meteorol.*, *18*, 479-486, 1961.

Danielsen, E., and V. Mohnen, Project Dustorm report: Ozone transport, in situ measurements, and meteorological analyses of tropopause folding, *J. Geophys. Res.*, *82*, 5867-5877, 1977.

Danielsen, E. F., R. S. Hipskind, S. E. Gaines, G. W. Sachse, G. L. Gregory, and G. F. Hill, Three-dimensional analysis of potential vorticity associated with tropopause folds and observed variations of ozone and carbon monoxide, *J. Geophys. Res.*, *92*, 2103-2111, 1987.

Davies, T. D., P. M. Kelly, P. S. Low, and C. E. Pierce, Surface ozone concentrations in Europe: Links with the regional-scale atmospheric circulation, *J. Geophys. Res.*, *97*, 9819-9832, 1992.

Dorling, S. R., T. D. Davies, and C. E. Pierce, A technique for estimating the synoptic meteorological controls on air and precipitation chemistry—Results from Eskdalemuir, South Scotland, *Atmos. Environ.*, *26(A)*, 2583-2602, 1992.

Feister, U., and K. Balzer, Surface ozone and meteorolog ical predictors on a subregional scale, *Atmos. Environ.*, *25(A)*, 1781-1790, 1991.

Haagenson, P. L., and M. A. Shapiro, Isentropic trajectories for derivation of objectively analyzed meteorological parameters, *NCAR Tech. Note, TN-149+STR*, 30+ pp., Natl. Cent. for Atmos. Res., Atmos. Qual. Div., Boulder, Colo., 1979.

Haagenson, P. L., and P. D. Sperry, A relationship of isentropic back trajectories with observed wind direction and synoptic type in the North Atlantic, *J. Appl. Meteorol.*, *28*, 25-42, 1989.

Harris, J. M., P. P. Tans, E. J. Dlugokencky, K. A. Masarie, P. M. Lang, S. W. Whittlestone, and L. P. Steele, Variations in atmospheric methane at Mauna Loa Observatory related to long-range transport, *J. Geophys. Res.*, *97*, 6003-6010, 1992.

Krishnamurti, T. N., H. E. Fuelberg, M. C. Sinha, D. Oosterhof, E. L. Bensman, and V. B. Kumar, The meteorological environment of the tropospheric ozone maximum over the tropical South Atlantic Ocean, *J. Geophys. Res.*, *98*, 10,621-10,641, 1993.

Kritz, M. A., S. W. Rosner, E. F. Danielsen, and H. B. Selkirk, Air mass origins and troposphere-to-stratosphere exchange associated with midlatitude cyclogenesis and tropopause folding inferred from $^7$Be measurements, *J. Geophys. Res.*, *96*, 17,405-17,414, 1991.

Levy, H., II, J. D. Mahlman, W. J. Moxim, and S. C. Liu, Tropospheric ozone: The role of transport, *J. Geophys. Res.*, *90*, 3753-3772, 1985.

Logan, J. A., Tropospheric ozone: Seasonal behavior, trends, and anthropogenic influence, *J. Geophys. Res.*, *90*, 10,463-10,482, 1985.

Logan, J. A., Ozone in rural areas of the United States, *J. Geophys. Res.*, *94*, 8511-8532, 1989.

Merrill, J., and W. C. Graustein, Large scale atmospheric transport patterns over the North Atlantic (abstract), *Eos Trans. AGU*, *70*, 1038, 1989.

Merrill, J. T., R. Bleck, and D. B. Boudra, Techniques of Lagrangian trajectory analysis in isentropic coordinates, *Mon. Weather Rev.*, *114*, 571-581, 1986.

Merrill, J. T., M. Uematsu, and R. Bleck, Meteorological analysis of long range transport to the Pacific Ocean, *J. Geophys. Res.*, *94*, 8584-8598, 1989.

Miller, J. M., J. L. Moody, J. M. Harris, and A. Gaudry, A 10-year trajectory flow climatology for Amsterdam Island, 1980-1989, *Atmos. Environ.*, *27(A)*, 1909-1916, 1993.

Moody, J. L., The influence of meteorology on precipitation chemistry at selected sites in the eastern United States, Ph.D. dissertation, 175 pp., Univ. of Mich., Univ. Microfilms Int., Ann Arbor, 1986.

Moody, J. L., and J. N. Galloway, Quantifying the relationship between atmospheric transport and the chemical composition of precipitation on Bermuda, *Tellus*, *40(B)*, 463-479, 1988.

Moody, J. L., and P. J. Samson, The influence of atmospheric transport on the composition of precipitation at two sites in the Midwestern United States, *Atmos. Environ*, *23*, 2117-2132, 1989.

Moody, J. L., A. A. P. Pszenny, A. Gaudry, W. C. Keene, J. N. Galloway, and G. Polian, Precipitation composition

and its variability in the southern Indian Ocean: Amsterdam Island, 1980-1987, *J. Geophys. Res.*, *96*, 20,769-20,786, 1991.

Oltmans, S. J., Surface ozone measurements in clean air, *J. Geophys. Res.*, *86*, 1174-1180, 1981.

Oltmans, S. J., and H. Levy II, Seasonal cycle of surface ozone over the western North Atlantic, *Nature*, *358*, 392-394, 1992.

Paluch, I. R., D. H. Lenschow, J. G. Hudson, and R. Pearson Jr., Transport and mixing processes in the lower troposphere over the ocean, *J. Geophys. Res.*, *97*, 7527-7542, 1992.

Parrish, D. D., C. J. Hahn, E. J. Williams, R. B. Norton, F. C. Fehsenfeld, H. B. Singh, J. D. Shetter, B. W. Gandrud, and B. A. Ridley, Indications of photochemical histories of Pacific air masses from measurements of atmospheric trace species at Point Arena, California, *J. Geophys. Res.*, *97*, 15,883-15,901, 1992.

Parrish, D. D., J. S. Holloway, M. Trainer, P. C. Murphy, G. L. Forbes, and F. C. Fehsenfeld, Export of North American ozone pollution to the North Atlantic Ocean, *Science*, *259*, 1436-1439, 1993.

Penkett, S. A., J. J. Blake, P. Lightman, A. R. W. March, P. Anwyl, and G. Butcher, The seasonal variation of nonmethane hydrocarbons in the free troposphere over the North Atlantic Ocean: Possible evidence for extensive reaction of hydrocarbons with the nitrate radical, *J. Geophys. Res.*, *98*, 2865-2886, 1993.

Pickering, K. E., et al., Free tropospheric ozone production following entrainment of urban plumes into deep convection, *J. Geophys. Res.*, *97*, 17,985-18,000, 1992.

Pickering, K. E., A. M. Thompson, D. P. McNamara, and M. R. Schoeberl, An intercomparison of isentropic trajectories over the South Atlantic, *Mon. Wea. Rev.*, *122*, 864-879, 1994.

Poirot, R. L., and P. R. Wishinsky, Visibility, sulfate and air mass history associated with the summertime aerosol in northern Vermont, *Atmos. Environ.*, *20*, 1457-1469, 1986.

Romesburg, C. H., *Cluster Analysis for Researchers*, 334 pp., Lifetime Learning, Belmont, Calif., 1984.

Samson, P. J., and J. L. Moody, Backward trajectories as two-dimensional probability fields, in *Air Pollution Modeling and its Applications: I*, edited by C. De Wispelaere, pp. 43-54, Plenum, New York, 1981.

Savoie, D. L., J. M. Prospero, S. J. Oltmans, W. C. Graustein, K. K. Turekian, J. T. Merrill, and H. Levy II, Sources of nitrate and ozone in the marine boundary layer of the tropical North Atlantic, *J. Geophys. Res.*, *97*, 11,575-11,589, 1992.

Shapiro, M. A., Turbulent mixing within tropopause folds as a mechanism for the exchange of chemical constituents between the stratosphere and troposphere, *J. Atmos. Sci.*, *37*, 994-1004, 1980.

Thompson, A. M., M. A. Huntley, and R. W. Stewart, Perturbations to tropospheric oxidants, 1985-2035, 1, Calculations of ozone and OH in chemically coherent regions, *J. Geophys. Res.*, *95*, 9829-9844, 1990.

Van Valin, C. C., and M. Luria, $O_3$, CO, hydrocarbons and dimethyl sulfide over the western Atlantic Ocean, *Atmos. Environ.*, *22*, 2401-2409, 1988.

Wakamatsu, S., I. Uno, H. Ueda, and K. Uehara, Observational study of stratospheric ozone intrusions into the lower troposphere, *Atmos. Environ.*, *23*, 1815-1826, 1989.

Walpole, R. E., and R. H. Myers, *Probability and Statistics for Engineers and Scientists*, 580 pp., Macmillan, New York, 1978.

H. Levy II, National Oceanic and Atmospheric Administration, GFDL, Princeton University, NJ 08540.

J. T. Merrill, Graduate School of Oceanography, University of Rhode Island, Narragansett, RI 02881.

J. L. Moody, Department of Environmental Sciences, University of Virginia, Clark Hall, Charlottesville, VA 22903.

S. J. Oltmans, National Oceanic and Atmospheric Administration, CMDL, Boulder, CO 80303.